Growth behavior of Al-doped zinc oxide microrods with times

Kyung Ho Kim*, Tomoyuki Umakoshi, Yoshio Abe, Midori Kawamura, Takayuki Kiba

Department of Materials Science and Engineering, Kitami Institute of Technology, 165 Koen-cho, Kitami, Hokkaido 090-8507, Japan

Abstract

We investigated the growth behavior of Al-doped zinc oxide (ZnO) microrods grown on ZnO seed layers at various growth times. During the initial 3 h (region I), the randomly oriented microrods grew on the surface of the substrate because of the weak acidity of the initial solution (pH ~5.5). Between 3 h and 6 h (region II), when the pH was close to neutrality, a dominant growth of Al-doped ZnO (AZO) microrods with tapered shape occurred. After that the vertical growth of the microrods reached a certain equilibrium, a selective etching of the side nonpolar plane, rather than the top polar plane, dominantly occurred between 6 h to 12 h (region III), thus leading to the formation of the microrods of cylindrical shape. From 12 h to 24 h (region IV), the pH value was saturated, and the

morphology of the microrods did not significantly change. As a result, owing to the change of the pH value, the growth behavior of the AZO microrods appeared significantly different when increasing the time.

Keywords: ZnO; Microrods; Growth; Morphology; Time; pH

*__Corresponding author.__ Tel.: +81 157 26 9431; fax: +81 157 26 4973, E-mail address: khkim@mail.kitami-it.ac.jp (K.H. Kim)

1. Introduction

One dimensional (1D) zinc oxide (ZnO) nano and microrods have been considered as one of the most promising material for the fabrication of novel nano and microscale electronic and optoelectronic devices [1-5]. The characteristics of nano and microrods are strongly related to the growth conditions (temperature [6,7], time [7-9], doping [8,10-12], pH [4,7,13,14], etc.). J. Sun et al. reported that nano and micro morphological changes occurred in ZnO by controlling the thickness of the seed layer [15]. Z. Zheng et al. found that the morphologies of ZnO grown on Pt-coated Si substrates changed from nanorods to microrods with and without Al [16].

In our previous study, we investigated the structural and optical properties of ZnO nanorods doped with Cu, Ag, and Al [11]. Compared with the undoped ZnO nanorods, the Cu-doped ZnO (CZO) nanorods exhibited increased length and improved crystallinity. On the other hand, Ag dopant led to a considerably opposite behavior. Interestingly, the incorporation of Al dopant in the ZnO led to a marked morphological variation with randomly oriented microrods, instead of nanorods, on the surface of the substrate. This morphological change of the ZnO nanorods with the addition of the Al dopant has been rarely reported. On the other hand, S. Kim et al. showed that, compared with the undoped ZnO nanorods, the length and diameter of Al-doped ZnO (AZO)

nanorods decreased and increased, respectively [10]. However, T-H. Fang and S-H. Kang reported an increased length and decreased diameter of the nanorods upon incorporation of Al [17]. The characteristics of ZnO nanorods doped with Al are still controversial and not fully understood. In this study, we investigated the growth behavior of the AZO microrods at various growth times.

2. Experimental

ZnO seed layers were prepared on the fluorine doped tin oxide (FTO) coated glass substrate by sol-gel spin-coating method using zinc acetate dihydrate ($Zn(CH_3CO)_2 \cdot 2H_2O$, 0.25 M) dissolved in 2-methoxyethanol (ME) ($C_3H_8O_2$), ethanol (C_2H_6O), and Milli-Q. A detailed description of the synthesis process has been previously reported elsewhere [12].

The AZO microrods were fabricated by chemical solution deposition with an aqueous solution of zinc nitrate hexahydrate ($Zn(NO_3)_2 \cdot 6H_2O$, 0.01 M), hexamethylenetetramine (HMT) ($C_6H_{12}N_4$, 0.01 M), and aluminum nitrate nanohydrate ($Al(NO_3)_3 \cdot 9H_2O$, 1 mM) as dopant. The ZnO seed layers prepared on the FTO coated glass substrate were vertically immersed in the solution at 90 ºC for 3-24 h. The samples were washed with deionized water and then dried at 120 ºC for 10 min.

The surface morphologies were examined using field emission scanning electron microscopy (FESEM, JSM-6701F), while the crystal structures and orientations were analyzed using X-ray diffraction (XRD, Bruker, D8ADVANCE) with Cu Kα radiation.

3. Results and discussion

Fig. 1 shows the cross-sectional FESEM images of the AZO microrods grown on the FTO coated glass substrates for (a) 3 h, (b) 6 h, (c-e) 12 h, and (f) 24 h. The variation of the length and of the bottom and top diameters of the microrods with the growth time are shown in Fig. 2. During the initial 3 h (Fig. 1(a)), the rods are randomly inclined to the surface of the substrate but rod with a diameter of several nanometer cannot be observed on the surface of the FTO substrate, in contrast to the undoped ZnO nanorods shown in Fig. S1 of the Supporting Information [18]. The length and the bottom and top diameters of the rods are ~2.0 μm, ~0.8 μm, and ~0.5 μm, respectively. The microrods are slightly wider at the bottom and tapered at the top. By increasing the growth time to 6 h (Fig. 1(b)), the shape of the microrods remains similar to that of the rods observed in the 3 h sample; however, the length of the microrods dramatically increases to ~8.5 μm. The bottom and top diameters are ~1.8 μm and ~0.7 μm, respectively. From XRD pattern in Fig.S2, the diffraction peaks observed for the (100),

(002), (101), and (110) planes match the pattern of the hexagonal wurzite ZnO structure (JCPDS card 36-1451). By further increasing the growth time to 12 h (Fig. 1(c)), the length of the microrods reaches ~8.8 μm. Notably, the growth dominantly occurred between 3 h to 6 h, while the length of the microrods did not show significant change when the time increased from 6 h to 12 h. The bottom and top diameters are ~1.2 μm and ~1.1 μm, respectively. It is worthy to note that the bottom diameter decreases, compared with that of the microrods observed in the 6 h sample, thus leading to the formation of cylindrically shaped microrods with equivalent top and bottom diameters. Fig. 1 (d) and (e) show high-magnification images of the areas marked with dotted squares at the top and bottom of the microrod in the Fig. 1(c), respectively. The microrod clearly shows a hexagonal cross-section, as seen in Fig. 1(d). Even though, in the bottom area, the etching of the microrod, rather than the growth, prevalently occurred, the surface appears quite smooth, as show in Fig. 1(e). By further increasing the time to 24 h (Fig. 1(f), the morphology of the microrods did not exhibit significant changes, compared with that of the 12 h sample.

The pH value of the AZO solution was measured to explain the growth evolution of the microrods with time. Fig. 3 shows (a) the pH value and (b) a schematic illustration of the growth and etching processes of the microrod with increasing the time. As shown

in Fig. 3 (a), the pH value of the initial AZO solution is ~5.5. During the initial 3 h (region I), the ZnO seed layer could be partially etched because of the weak acidity of the solution, leading to the growth of randomly distributed microrods [4,13,15]. Between 3 h and 6 h (region II), the pH is close to neutrality and the microrods grow dramatically. In the region I and II, the growth process dominates, rather than the etching process; meanwhile, the growth rate in the region II is higher than that in the region I. Between 6 h to 12 h (region III), the pH value increases to ~7.8; interestingly, the etching of the side surface of the microrods in the bottom area can be observed along with the growth of the side surface in the top area, thus leading to formation of the microrods of cylindrical shape rather than tapered shape, as illustrated in Fig. 3(b). This phenomenon appears quite different from the typical etching process of ZnO along preferential directions. It was reported that the etching rate of the polar top plane is higher than that of the nonpolar side surface planes, which leads to the hollow nanotube structure in the selective self-etching mechanism [19-21]. A fast etching process of the side surface might indicate that the AZO microrods with a tapered shape have the more defects on the side surface in the bottom area than on the top plane [20]. Moreover, a further increase of the time to 24 h (region IV) saturates the pH value; the AZO microrods remain quite stable and maintain their cylindrical shape.

4. Conclusions

We studied the effects of the growth time on the growth behavior of the AZO microrods grown on a ZnO seed layer using chemical solution deposition. By increasing the time, the pH value increased and saturated at ~7.8. Owing to the weak acidity of the initial AZO solution, randomly oriented microrods grew on the surface of the substrate. From 3 h to 6 h, with the pH close to neutrality, the growth of the microrods prevailed on the etching process. From 6 h to 12 h, the diameter of the microrods gradually decreased from bottom to top. The selective etching and growth of microrods with bottom-wise tapered shape led to the formation of cylindrically shaped microrods. From 12 h to 24 h, with the saturation of the pH, no significant morphological change of the microrods was observed.

References

[1] Ü. Özgür, Y.I. Alivov, C. Liu, A. Teke, M.A. Reshchikov, S. Doğan, V. Avrutin, S.-J. Cho, H. Morkoç, A comprehensive review of ZnO materials and devices, J. Appl. Phys. 98 (2005) 041301-1-103.

[2] J. Bao, M.A. Zimmler, F. Capasso, X. Wang, Z.F. Ren, Z.F. Ren, Broadband ZnO single-nanowire light-emitting diode, Nano. Lett. 6 (2006) 1719-1722.

[3] J.H. Kim, D. Andeen, F.F. Lange, Hydrothermal growth of periodic, single-crystal ZnO microrods and microtunnels, Adv. Mater. 18 (2006) 2453-2457.

[4] X. Yan, Z. Li, R. Chen, W. Gao, Template growth of ZnO nanorods and microrods with controllable densities, Cryst. Growth Des. 8 (2008) 2406-2410.

[5] A. Kolodziejczak-Radzimska, T. Jesionowski, ZnO oxide-From synthesis to application:A review, Materials 7 (2014) 2833-2881.

[6] S. Zhang, C. Yan, H. Zhang, G. Lu, Effects of bath temperature on the morphology of ZnO nano-rods and its optical properties, Mater. Lett. 148 (2015) 1-4.

[7] G. Amin, M.H. Asif, A. Zainelabdin, S. Zaman, O. Nur, M. Willander, Influence of pH, precursor concentration, growth time, and temperature on the morphology of ZnO nanostructures grown by the hydrothermal method, J. Nanomater. Volume 2011, Article ID 269692.

[9] D. Polsongkram, P. Chamninok, S. Pukird, L. Chow, O. Lupan, G. Chai, H. Khallaf, S. Park, A. Schulte, Effect of synthesis conditions on the growth of ZnO nanorods via hydrothermal method, Physica B 403 (2008) 3713-3717.

[9] L. Zhang, X. Liu, C. Geng, H. Fang, Z. Lian, X. Wang, D. Shen, Q. Yan, Hexagonal crown-capped zinc oxide micro rods: Hydrothermal growth and formation mechanism, Inorg. Chem. 52 (2013) 10167-10175.

[10] S. Kim, G. Nam, H. Park, H. Yoon, S-h. Lee, J.S. Kim, J.S. Kim, D.Y. Kim, S-O. Kim, J-Y. Leem, Effects of doping with Al, Ga, and In on structural and optical properties of ZnO nanorods grown by hydrothermal method, Bull Korean Chem. Soc. 34 (2013) 1205-1211.

[11] K.H. Kim, Z. Jin, Y. Abe, M. Kawamura, Structural and optical properties of Cu-Ag, and Al-doped zinc oxide nanorods, Superlattice. Microst. 75 (2014) 455-460.

[12] K.H. Kim, Z. Jin, Y. Abe, M. Kawamura, Effects of Li and Cu dopants on structural properties of zinc oxide nanorods, Superlattice. Microst. 77 (2015) 101-107.

[13] Y. Liu, W. Gao, Growth process, crystal size and alignment of ZnO nanorods synthesized under neutral and acid conditions, J. Alloy. Compd. 629 (2015) 84-91.

[14] L.L. Yang, Q.X. Zhao, M. Willander, Size-controlled growth of well-aligned ZnO nanorod arrays with two-step chemical bath deposition method, J. Alloy. Compd. 469

(2009) 623-629.

[15] J. Sun, J. Bian, L. Chen, Y. Wang, Y. Gong, Y. Li, K. Liu, C. Chang, M. Li, G. Du, Realization of wide size range 1D ZnO micro/nano rods for versatile micro/nanodevices by controlled seed layer thickness, Appl. Surf. Sci. 276 (2013) 782-786.

[16] Z. Zheng, Z.S. Lim, Y. Peng, L. You, L. Chen, J. Wang, General route to ZnO nanorod arrays on conducting substrates via galvanic-cell-based approach, Scientific Reports 3 (2013) 2434.

[17] T-H. Fang, S-H. Kang, Surface and physical characteristics of ZnO:Al nanostructured films, J. Appl. Phys. 105 (2009) 113512-1-113512-8.

[18] Z. Jin, T. Umakoshi, Y. Abe, M. Kawamura, K.H. Kim, Effect of Cu dopant on structural and optical properties of zinc oxide nanorods, The 21st International Display Workshops (IDW), Niigata, Japan, FMCp4-1, 2014.

[19] F. Li, Y. Ding, P. Gao, X. Xin, Z.L. Wang, Single-crystal hexagonal disks and rings of ZnO: Low-temperature, large-scale synthesis and growth mechanism, Angew Chem. Int. Ed 43 (2004) 5238-5242.

[20] G-W. She, X-H. Zhang, W-S. Shi, X. Fan, J.C. Chang, C-S. Lee, S-T. Lee, C-H. Liu, Controlled synthesis of oriented single-crystal ZnO nanotube arrays on transparent conductive substrates, Appl. Phys. Lett. 92 (2008) 053111-1-053111-3.

[21] B-R. Huang, J-C. Lin, A facile synthesis of ZnO nanotubes and their hydrogen sensing properties, Appl. Surf. Sci. 280 (2013) 945-949.

Figure captions

Fig. 1. Cross-sectional FESEM images of AZO microrods with growth time of (a) 3 h, (b) 6 h, (c-e) 12 h, and (f) 24 h; (d,e) high-magnification images of the areas marked with dotted squares at the top and bottom regions in (c).

Fig. 2. Length (circle), and bottom (square) and top (triangle) diameters of AZO microrods as functions of the growth time.

Fig. 3. (a) pH value vs growth time and (b) schematic illustration of the microrod growth and etching processes.

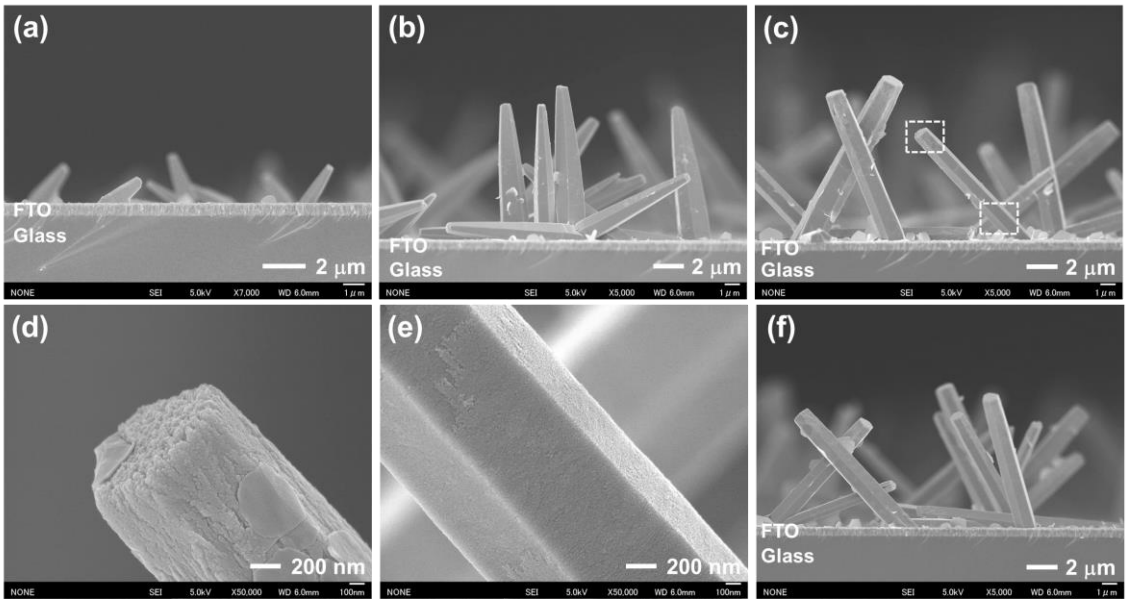
(a)
FTO
Glass
2 μm
(b)
FTO
Glass
2 μm
(c)
FTO
Glass
2 μm
(d)
200 nm
(e)
200 nm
(f)
FTO
Glass
2 μm

Fig. 1.

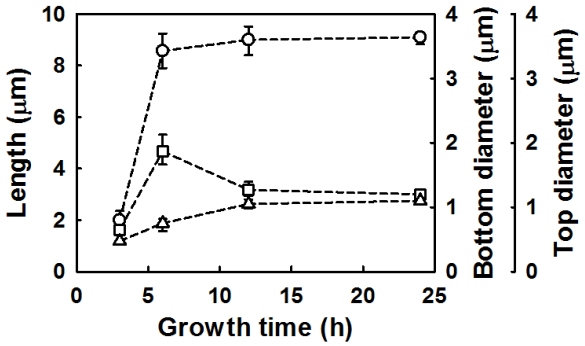
Length (μm)
Bottom diameter (μm)
Top diameter (μm)
Growth time (h)
0
2
4
6
8
10
0
1
2
3
4
0
5
10
15
20
25

Fig. 2.

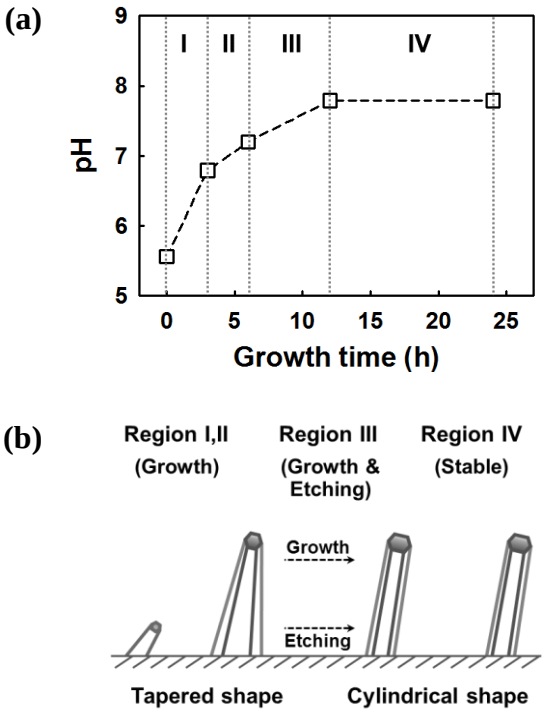
(a)
9
8
7
6
5
pH
I
II
III
IV
0
5
10
15
20
25
Growth time (h)
(b)
Region I,II
(Growth)
Region III
(Growth &
Etching)
Region IV
(Stable)
Growth
Etching
Tapered shape
Cylindrical shape

Fig. 3.